Swing-Up and Stabilization of a Cart Pendulum System and Stabilization of a Twin Pendulum System

Using Nonlinear Control Strategies

Master Thesis

Aalborg University
Control & Automation
Fredrik Bajers Vej 7
DK-9220 Aalborg

by
Niels Skov Vestergaard

AALBORG UNIVERSITY
STUDENT REPORT

Master Thesis

Control and Automation

Department of Electronic Systems

Fredrik Bajers Vej 7C

9220 Aalborg

Title:
Swing-Up and Stabilization of a Cart Pendulum System and Stabilization of a Twin Pendulum System

Subtitle:
Using Nonlinear Control Strategies

Theme:
Nonlinear Control

Project Period:
Autumn 2018

Participants:
Niels Skov Vestergaard

Supervisor:
John-Josef Leth

Pages: ?
Appendices: ?
Attachments: ?

Concluded: 2019-01-16

Synopsis:

Nam dui ligula, fringilla a, euismod sodales, sollicitudin vel, wisi. Morbi auctor lorem non justo. Nam lacus libero, pretium at, lobortis vitae, ultricies et, tellus. Donec aliquet, tortor sed accumsan bibendum, erat ligula aliquet magna, vitae ornare odio metus a mi. Morbi ac orci et nisl hendrerit mollis. Suspendisse ut massa. Cras nec ante. Pellentesque a nulla. Cum sociis natoque penatibus et magnis dis parturient montes, nascetur ridiculus mus. Aliquam tincidunt urna. Nulla ullamcorper vestibulum turpis. Pellentesque cursus luctus mauris.
Nam dui ligula, fringilla a, euismod sodales, sollicitudin vel, wisi. Morbi auctor lorem non justo. Nam lacus libero, pretium at, lobortis vitae, ultricies et, tellus. Donec aliquet, tortor sed accumsan bibendum, erat ligula aliquet magna, vitae ornare odio metus a mi. Morbi ac orci et nisl hendrerit mollis. Suspendisse ut massa. Cras nec ante. Pellentesque a nulla. Cum sociis natoque penatibus et magnis dis parturient montes, nascetur ridiculus mus. Aliquam tincidunt urna. Nulla ullamcorper vestibulum turpis. Pellentesque cursus luctus mauris.

Contents

1 | Introduction

This project is concerned with developing nonlinear control strategies for a cart pendulum system and to apply these to the set-up provided in the Control and Automation Lab at Aalborg University (AAU).
The project is two part. The objective of the first part is to design a swing-up controller along with a stabilizing controller to catch the pendulum at the upright position.
In the second part an additional pendulum is attached to the cart in the setup making it a twin pendulum system. The idea is to estimate the additional state and ultimately stabilize the two pendulums in upright position.

Part I

Cart Pendulum

2 | System and Model

A brief overview of the relevant system for *Part 1* is presented in this chapter along with a model of the system.

2.1 System

A setup is provided by the Control and Automation Department at AAU, see Figure 2.1.

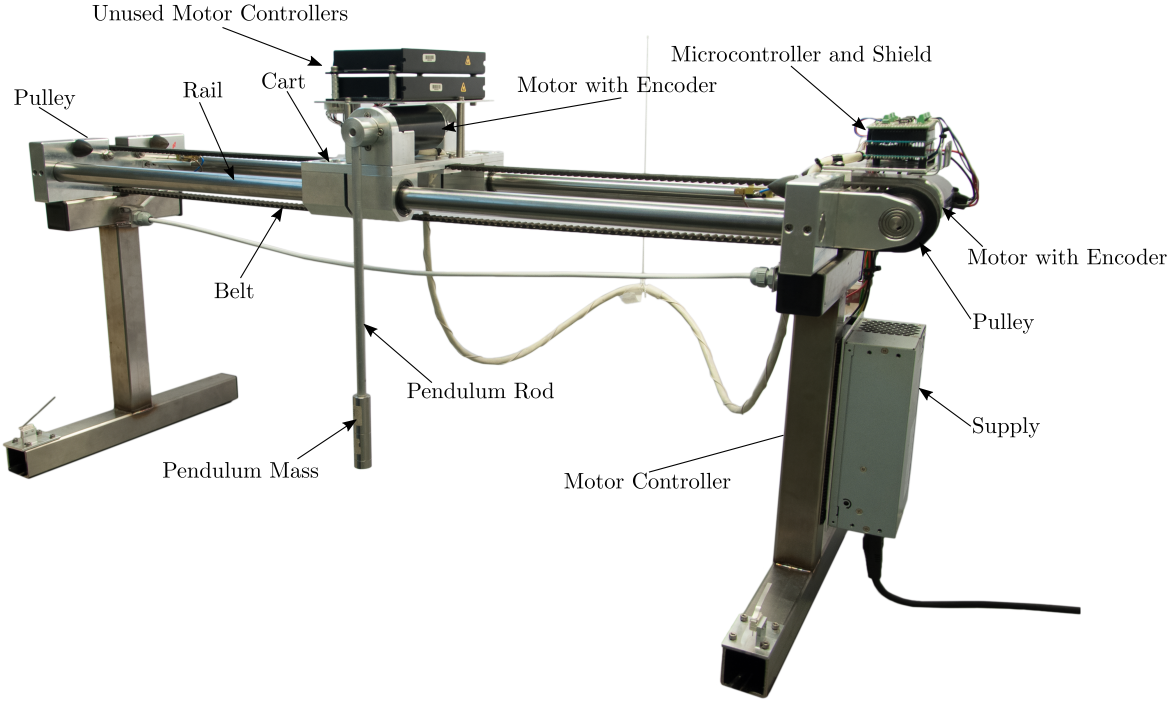

Figure 2.1: The setup provided by AAU. The motor controller in use is not directly visible in this picture as it is mounted behind the power supply.

As seen in Figure 2.1 the belt is attracted by pulleys one of which is driven by a brushed Maxon 370356 DC motor [1]. An other of these maxon motors is mounted on the pendulum but is disconnected and just used as a bearing in this project. Both motors are fitted with an HEDS 5540 optical quadrature encoder allowing for relative position and angle of the cart and pendulum respectively [2].

The motor driving the belt is controlled using a Maxon ADS 50/10 motor controller configured in current control mode. The motor controller takes a $\pm 10\,\mathrm{V}$ input signal which then determines the armature current, i_a, see [3].

The primary control unit is a Teensy 3.6 microcontroller board. To program the board through the onboard USB connection a bootloader is used along with the Teensyduino add-on for the Arduino IDE [4].

The encoders are decoded on a shield using Avago HCTL-2021-PLC decoders and read through an 8 bit parallel data bus on the microcontroller board resulting in 2000 tics pr. revolution. This ensures a resolution for the pendulum angle, θ, of $2\pi/2000 = \pi \times 10^{-3}\,\mathrm{rad/tic}$ and $2\pi r/2000 = 2\pi \cdot 0.028/2000 \approx 0.088 \times 10^{-3}\,\mathrm{m/tic}$ for the cart position, x, see [5].

The supply circuit on the microcontroller board is powered by 5V which is regulated to 3.3 V resulting in a 0−3.3 V range for the 12 bit analog output [6]. This output is used to provide the motor controller with an armature current reference, thus, the microcontroller analog output is amplified through the shield to meet the ±10 V input requirement of the motor controller [7].

The following relation between analog 12 bit output values, $\mathrm{bit}_{\mathrm{DAC}}$, from the microcontroller and armature current in the motor was found by a previous project group [7],

$$\mathrm{bit}_{\mathrm{DAC}} = 105.78 \cdot i_a + 1970 \quad , \tag{2.1}$$

and as a result of a force test, see [8], Equation 2.1 was corrected to,

$$\mathrm{bit}_{\mathrm{DAC}} = 111.9 \cdot i_a + 1970 \quad , \tag{2.2}$$

which is the relation used in this project. All the system parameters used in the design are listed in Table 2.1. It is assumed that all frictions in the system can be modeled as a combination of Coulomb and viscous frictions. Wires hanging from the cart are unmodeled and their weight along with that of the belt are contained in the estimation of the cart mass.

Parameter	**Notation**	**Quantity**	**Unit**
Nominal current (max. continuous current)	I_{N}	4.58	A
Torque constant	τ_m	93.4×10^{-3}	$\mathrm{N \cdot m \cdot A^{-1}}$
Rod Length	l	0.3235	m
Rail Length	l_r	0.89	m
Pulley Radius	r	0.028	m
Pendulum Mass	m	0.201	kg
Cart Mass	M	5.273	kg
Cart Coulomb Friction	$b_{c,c}$	2.884	N
Cart Viscous Friction	$b_{c,v}$	1.680	$\mathrm{N{\cdot}m^{-1}{\cdot}s}$
Pendulum Coulomb Friction	$b_{p,c}$	0.004	N·m
Pendulum Viscous Friction	$b_{p,v}$	0.4×10^{-3}	N·m·s

Table 2.1: The motor parameters, I_{N} and τ_m, are given by maxon in [1]. The rod length is measured from the pendulum pivot point to the geometrical center of the pendulum. Pendulum mass, rod length, pulley radius and rail length are measured parameters, while cart mass is estimated same as all frictions. The estimations are performed by a previous project group [7].

2.2 Model

The model is based on the generalized coordinates presented in Figure 2.2.

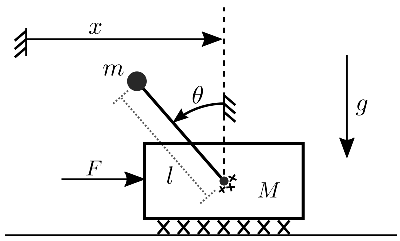

Figure 2.2: Mechanical drawing of the system, where θ is the angle of the pendulum, x is the position of the center of the cart along the rail, F is the applied force and g is the gravitational acceleration. It is indicated that friction is modeled between cart and rail as well as in the pendulum joint.

The pendulum mass center is positioned at zero hight at rest s.t. all energies in the system are positive. It is assumed that the pendulum rod is rigid and massless and that the pendulum weights are a point mass at the geometrical center of the weights.
The motor torque is given by direct relation to the armature current by the motor constant, $\tau_m = k_\tau i_a$, such that,

$$F = \frac{1}{r} k_\tau i_a \qquad \text{[N]} \tag{2.3}$$

It is well known that the potential energy, U, and the kinetic energy, T, are given by, [9]

$$U = mgl(1 + \cos\theta) \qquad [\mathrm{J}] \tag{2.4}$$

$$T = \frac{1}{2}(M+m)\dot{x}^2 - m\dot{x}l\cos\theta\dot{\theta} + \frac{1}{2}ml^2\dot{\theta}^2 \quad . \qquad [\mathrm{J}] \tag{2.5}$$

The frictions, indicated in Figure 2.2, are, as mentioned, comprised of Coulomb and viscous frictions with values stated in Table 2.1. The viscous frictions are modeled as linear functions of velocities, [10, 11]

$$b_{p,v}\dot{\theta} \quad , \quad b_{c,v}\dot{x} \quad , \tag{2.6}$$

for the rotational and linear case respectively. The coulomb frictions are modeled as a constant with its sign depending on the signs of the velocities, such that, [10, 11]

$$\mathrm{sgn}(\dot{\theta})b_{p,c} \quad , \quad \mathrm{sgn}(\dot{x})b_{c,c} \quad . \tag{2.7}$$

This, however, introduces discontinuities at zero velocities. Thus, tanh-functions are used to obtain a continues approximation of the sign-functions,

$$\tanh(\mathrm{k_{tanh}}\dot{\theta})b_{p,c} \quad , \quad b_{c,v}\dot{x} - \tanh(\mathrm{k_{tanh}}\dot{x})b_{c,c} \quad , \tag{2.8}$$

where $\mathrm{k_{tanh}} = 250$ to increase the steepness of the tanh-functions thereby obtaining a closer approximation of the sign-functions. Finally, by use of the Lagrange-d'Alembert Principle, [9]

$$\frac{d}{dt}\frac{\partial \mathcal{L}}{\partial \dot{\mathbf{q}}} - \frac{\partial \mathcal{L}}{\partial \mathbf{q}} = \mathbf{Q} \quad , \tag{2.9}$$

where,

$$\mathbf{q} = \begin{bmatrix} \theta \\ x \end{bmatrix} \quad , \quad \mathbf{Q} = \begin{bmatrix} -b_{p,v}\dot{\theta} - \tanh(\mathrm{k_{tanh}}\dot{\theta})b_{p,c} \\ \frac{1}{r}k_\tau i_a - b_{c,v}\dot{x} - \tanh(\mathrm{k_{tanh}}\dot{x})b_{c,c} \end{bmatrix} \quad , \tag{2.10}$$

and $\mathcal{L} = T - U$, the dynamics of the system are found,

$$ml^2\ddot{\theta} - ml\cos\theta\ddot{x} - mgl\sin\theta = -b_{p,v}\dot{\theta} - \tanh(\mathrm{k_{tanh}}\dot{\theta})b_{p,c} \qquad [\mathrm{N\cdot m}] \tag{2.11}$$

$$(M+m)\ddot{x} + ml\sin\theta\dot{\theta}^2 - ml\cos\theta\ddot{\theta} = F - b_{c,v}\dot{x} - \tanh(\mathrm{k_{tanh}}\dot{x})b_{c,c} \quad . \qquad [\mathrm{N}] \tag{2.12}$$

By setting up the dynamic equations, Equation 2.12 and 2.11, in the following manner,

$$\begin{aligned} &\begin{bmatrix} ml^2 & -ml\cos\theta \\ -ml\cos\theta & M+m \end{bmatrix} \begin{bmatrix} \ddot{\theta} \\ \ddot{x} \end{bmatrix} + \begin{bmatrix} 0 \\ ml\sin\theta\dot{\theta}^2 \end{bmatrix} + \\ &+ \begin{bmatrix} b_{p,v}\dot{\theta} + \tanh(\mathrm{k_{tanh}}\dot{\theta})b_{p,c} \\ b_{c,v}\dot{x} + \tanh(\mathrm{k_{tanh}}\dot{x})b_{c,c} \end{bmatrix} + \begin{bmatrix} -mgl\sin\theta \\ 0 \end{bmatrix} = \begin{bmatrix} 0 \\ F \end{bmatrix} \quad , \end{aligned} \tag{2.13}$$

the general form of an m-link robot is obtained, [12, 13]

$$\mathbf{M}(\mathbf{q})\ddot{\mathbf{q}} + \mathbf{C}(\mathbf{q}, \dot{\mathbf{q}}) + \mathbf{B}(\dot{\mathbf{q}}) + \mathbf{G}(\mathbf{q}) = \mathbf{F} \quad , \tag{2.14}$$

where,

$\mathbf{M}(\mathbf{q})$	is the inertia matrix
$\mathbf{C}(\mathbf{q}, \dot{\mathbf{q}})$	is the Coriolis and centrifugal effects
$\mathbf{B}(\dot{\mathbf{q}})$	is the friction
$\mathbf{G}(\mathbf{q})$	is the force due to gravity
$\mathbf{F}$	is the input force

3 | Swing-Up Design

In this chapter a swing-up controller is designed based on [14]. The pendulum is started at rest, $\theta = \pi$, angle convention is specified in Figure 2.2. The idea of the swing-up controller is to increase the mechanical energy in the system until it matches that of the desired end state, which is the upright position at rest, that is, $\theta = 0$ and $\dot{\theta} = 0$. The minimum energy in the system is the starting position at rest, which is considered to be zero as mentioned in the *Model* section 2.2. So the target energy is $E_{\text{eq}} = 2mgl$, that is, the potential energy of the pendulum in the unstable equilibrium.

Consider the pendulum dynamics from Equation 2.12,

$$J\ddot{\theta} - ml\cos\theta\ddot{x}_c - mgl\sin\theta = 0 \quad , \qquad [\text{N} \cdot \text{m}] \tag{3.1}$$

where $J = ml^2$ is the inertia and the pendulum friction is assumed to be zero. This equation captures the behavior of the pendulum corresponding to some acceleration $\ddot{x}_c$ at the pivot point. This acceleration is viewed as the control input for now. The force needed to achieve this acceleration is considered in the end of the design. It is further convenient to describe the energy of the pendulum with the coordinate frame fixed at its pivot point, see Figure 3.1.

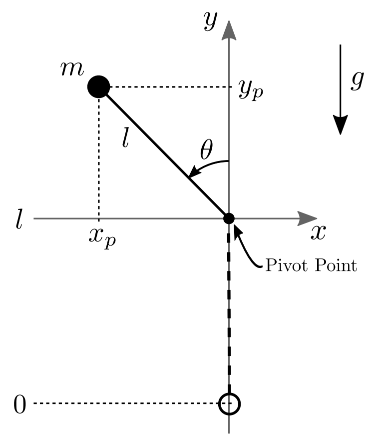

Figure 3.1: The energy used in the swing-up controller is described using this convention, where the coordinate frame is fixed at the pivot point of the pendulum. The zero reference is placed as before s.t. all energies are positive.

From Figure 3.1, the conversion from excessive to generalized coordinates is given by,

$$x_p = -l\sin\theta \quad , \quad y_p = l(\cos\theta + 1) \quad , \quad \dot{x}_p = -l\cos\theta\dot{\theta} \quad , \quad \dot{y}_p = -l\sin\theta\dot{\theta} \quad . \tag{3.2}$$

The mechanical energy in this coordinate frame is then,

$$E_p = mgy_p + \tfrac{1}{2}m\dot{x}_p^2 + \tfrac{1}{2}m\dot{y}_p^2 \qquad \text{[J]} \tag{3.3}$$
$$E_p = mgl(\cos\theta + 1) + \tfrac{1}{2}m(-l\cos\theta\dot{\theta})^2 + \tfrac{1}{2}m(-l\sin\theta\dot{\theta})^2 \qquad \text{[J]} \tag{3.4}$$
$$E_p = mgl(\cos\theta + 1) + \tfrac{1}{2}J(\cos^2\theta + \sin^2\theta)\dot{\theta}^2 \qquad \text{[J]} \tag{3.5}$$
$$E_p = \tfrac{1}{2}J\dot{\theta}^2 + mgl(\cos\theta + 1) \quad . \qquad \text{[J]} \tag{3.6}$$

A Lyapunov function candidate is proposed,

$$V = \tfrac{1}{2}E_\Delta^2 \quad , \tag{3.7}$$

where E_Δ is the difference in energy in relation to the unstable equilibrium,

$$E_\Delta = E_p - E_{\mathrm{eq}} \qquad \text{[J]} \tag{3.8}$$
$$E_\Delta = \tfrac{1}{2}J\dot{\theta}^2 + mgl(\cos\theta + 1) - 2mgl \qquad \text{[J]} \tag{3.9}$$
$$E_\Delta = \tfrac{1}{2}J\dot{\theta}^2 + mgl(\cos\theta - 1) \quad . \qquad \text{[J]} \tag{3.10}$$

The derivative of E_Δ from Equation 3.10 along the system Equation 3.1 is found to,

$$\dot{E}_\Delta = J\dot{\theta}\ddot{\theta} - mgl\sin\theta\dot{\theta} \tag{3.11}$$
$$\dot{E}_\Delta = \dot{\theta}(ml\cos\theta\ddot{x}_c + mgl\sin\theta) - mgl\sin\theta\dot{\theta} \tag{3.12}$$
$$\dot{E}_\Delta = ml\cos\theta\dot{\theta}\ddot{x}_c \quad . \tag{3.13}$$

The Lyapunov function candidate, Equation 3.7, is continuously differentiable in the entire $\mathbb{R}^2$ [1]. Its derivative is evaluated to find a stabilizing controller,

$$\dot{V} = E_\Delta\dot{E}_\Delta \tag{3.14}$$
$$\dot{V} = E_\Delta ml\cos\theta\dot{\theta}\ddot{x}_c \leq 0 \quad . \tag{3.15}$$

The acceleration, $\ddot{x}_c$, is then designed to satisfy the stability criterion in Equation 3.15,

$$\dot{V} = mlE_\Delta\cos\theta\dot{\theta}(-E_\Delta\cos\theta\dot{\theta}) \tag{3.16}$$
$$\dot{V} = -ml(E_\Delta\cos\theta\dot{\theta})^2 \leq 0 \quad , \tag{3.17}$$

further a tuning parameter, $k > 0$, is introduced such that the control law for acceleration of the pivot point is,

$$\ddot{x}_c = -kE_\Delta\cos\theta\dot{\theta} \quad . \tag{3.18}$$

[1] FiXme Note: brush up on stability criteries

Part II

Twin Pendulum

Bibliography

[1] *Maxon Motor*. Aug. 15, 2018. URL: https://www.maxonmotor.com/maxon/view/product/motor/dcmotor/re/re50/370356.

[2] Avago Technologies. *HEDM-55xx/560x & HEDS-55xx/56xx*. Aug. 15, 2018. URL: https://www.infineon.com/dgdl/Infineon-Encoder_HEDS-5540-A14-AP-v01_00-EN.pdf?fileId=5546d46147a9c2e40147d3d593970357.

[3] *Maxon Controller*. Aug. 15, 2018. URL: https://www.maxonmotor.com/maxon/view/product/control/Servoverstaerker-4-Q-DC/201583.

[4] *sparkfun Teensy 3.6*. Aug. 15, 2018. URL: https://www.sparkfun.com/products/14057.

[5] *HCTL-2021 PLC Avago Datasheet*. Aug. 15, 2018. URL: https://datasheet.octopart.com/HCTL-2021-PLC-Avago-datasheet-7580518.pdf.

[6] *K66 Sub-Family Reference Manual*. Aug. 15, 2018. URL: https://cdn.sparkfun.com/datasheets/Dev/Arduino/Boards/K66P144M180SF5RMV2.pdf.

[7] Jonas Ørndrup Jesper H. Hørgensen. *Non-linear Control and Machine Learning on an Inverted Pendulum on a Cart. Master Thesis*. 2018.

[8] Niels Skov Vestergaard. *Sliding Mode Stabilization and Phase Plane Trajectory Planning for a Cart Pendulum System. 9th Semester Project*. 2018.

[9] Rafael Wisniewski. *Mechanical Systems II. Lagrange Mechanics*. Aalborg University, 2013.

[10] Charles M. Close, Dean K. Frederick, and Jonathan C. Newell. *Modeling and Analysis of Dynamic Systems*. Wiley, 2001.

[11] H. Olsson et al. *Friction Models and Friction Compensation*. Nov. 28, 1997.

[12] Mark W. Spong, Seth Hutchinson, and M. Vidyasagar. *Robot Dynamics and Control*. 2nd ed. Wiley, 2005.

[13] Lorenzo Sciavicco and Bruno Siciliano. *Modelling and Control of Robot Manipulators*. 2nd ed. Lorenzo Sciavicco and Bruno Siciliano. London: Springer, 2012.

[14] Karl Johan Åström and Katsuhisa Furuta. “Swinging up a pendulum by energy control”. In: *Automatica* 36.2 (2000), pp. 287–295.

List of Corrections